Effect of lead additive on the ferroelectric properties and microstructure of Sr x Pb y Bi 2z Ta 2 O 9 thin films

San-Yuan Chen and Ving-Ching Lee

Citation: Journal of Applied Physics **87**, 8024 (2000); doi: 10.1063/1.373491
View online: http://dx.doi.org/10.1063/1.373491
View Table of Contents: http://scitation.aip.org/content/aip/journal/jap/87/11?ver=pdfcov
Published by the AIP Publishing

Effect of lead additive on the ferroelectric properties and microstructure of $Sr_xPb_yBi_{2z}Ta_2O_9$ thin films

San-Yuan Chen[a] and Ving-Ching Lee
Department of Materials and Science Engineering, National Chiao-Tung University, 300 Hsinchu, Taiwan, People's Republic of China

(Received 30 November 1999; accepted for publication 21 February 2000)

Ferroelectric thin films of bismuth-containing layered perovskite $Sr_xPb_yBi_{2z}Ta_2O_9$ have been prepared using the metalorganic decomposition method. The effect of both Sr and Pb content on the crystal structure, microstructure, and ferroelectric properties of $Sr_xPb_yBi_{2.3}Ta_2O_9$ films was investigated. A maximum remanent polarization of $2P_r = 19.2\,\mu C/cm^2$ was obtained for the $Sr_xPb_{0.2}Bi_{2.3}Ta_2O_9$ film with 20 mol % Sr-deficient composition as prepared at 800 °C, which could be the compromising effects of Sr content on both grain growth and second phase formation of $BiTaO_4$. The substitution of Pb for Bi is accompanied by the occurrence of oxygen vacancies to compensate the charge balance, which is responsible for grain growth mechanism in $Sr_{0.8}Pb_{0.2}Bi_{2.3}Ta_2O_9$ films. Fatigue endurance of $Sr_{0.8}Bi_{2.3}Ta_2O_9$ films becomes problematic after 10^9 cycles with a decrease in remanent polarization to 85% of the original value. This phenomenon was related to electron injection and creation of electron traps due to the occupation of Sr vacancies by Bi cations. It is demonstrated that the fatigue endurance of $Sr_{0.8}Bi_{2.3}Ta_2O_9$ film can be improved by doping with 20 mol % PbO. © *2000 American Institute of Physics.* [S0021-8979(00)01311-6]

I. INTRODUCTION

Bismuth-containing layered perovskites were found to be ferroelectric by Smolenskii *et al.*[1,2] They belong to the family of Aurivillius compounds with a general formula of $(Bi_2O_2)^{+2}(A_{m-1}B_mO_{3m+1})^{2-}$, consisting of m-perovskite units sandwiched between bismuth oxide layers. (Here A and B are the two types of cations that enter the perovskite unit. A is Bi^{+3}, Ba^{+2}, Sr^{+2}, Pb^{+2}, or K^{+1}; B is Ti^{4+}, Ta^{+5}, Nb^{5+}, Mo^{6+} or W^{6+}.)

Ferroelectric thin films of $SrBi_2Nb_2O_9$ (SBN), $SrBi_2Ta_2O_9$ (SBT) and their solid solutions are being widely investigated for applications in high density nonvolatile ferroelectric random access memories because of their excellent ferroelectric properties, characterized by limited polarization fatigue and low coercive field.[3,4] Various deposition methods have been used to produce Bi layer-structured ferroelectric thin films, such as rf sputtering,[5] laser ablation,[6] metalorganic chemical vapor deposition,[7] and wet-chemical processes [sol–gel or metalorganic decomposition (MOD)].[8–10]

Ferroelectric properties, crystal structure, and microstructure are remarkably influenced by the composition fluctuation in the bismuth layer structured compounds. Atsuki *et al.*[11] reported that the remanent polarization P_r of $Sr_xBi_{2z}Ta_2O_9 (0.7 \leqslant x \leqslant 1.0,\ 2.0 \leqslant 2z \leqslant 2.6)$ increased with the decrease of the Sr/Ta mole ratio for films annealed at 800 °C. A maximum remanent polarization was obtained for the 20 mol % Sr-deficient and 10 mol % Bi-excess composition.[12] Noguchi *et al.* attributed the enhancement in P_r with decreasing Sr content from $x = 1.0$ to 0.8 to the increase in grain growth. On the other hand, the decrease of P_r value with further decreasing Sr content is due to the disappearance of the SBT phase and the formation of a $BiTaO_4$ second phase.[13] On the other hand, Watanabe *et al.*[14] reported that the dependence of P_r on Sr content in SBN films was entirely due to the sensitivity of grain orientation to Sr content. The randomly oriented Sr-deficient SBN films have larger remanent polarization than *c*-axis oriented stoichiometric SBN films. An asymmetric hysteresis loop was also observed in Sr-deficient SBT films. Excess Bi is usually required to achieve stoichiometry due to the high volatility of Bi during processing[15] and Bi diffusion into the bottom electrode during annealing.[16] Watanabe *et al.*[17] reported that the SBT films grown with an excess bismuth of around 20% $(2z = 2.4)$ yields a maximum P_r value and a lower coercive field.

$PbBi_2Nb_2O_9$ is another ferroelectric compound that has a layered perovskite structure.[1] It has a pseudotetragonal unit cell with lattice parameters $a = 5.492$ Å, $b = 5.503$ Å, $c = 25.53$ Å, and $Z = 4$.[18] Subbarao *et al.*[19] found well-defined hysteresis loops for $PbBi_2Nb_2O_9$-based capacitors at 200 °C, but its relatively high coercive field made it difficult to obtain ferroelectric switching at room temperature.[20] From the viewpoint of the general formula of Aurivillius compounds, Pb, similar to Sr in the $SrBi_2Nb_2O_9$, occupies the *A* site in the perovskite unit of $PbBi_2Nb_2O_9$. However, Pb and Bi are known to have $6s^2$ lone pair electrons and tend to form layered structures, thus promoting strong ferroelectricity. A recent study by Millan *et al.*[21] reported that when the $SrBi_2Nb_2O_9$ ceramic was doped with PbO, the Pb^{2+} cation was incorporated into the orthorhombic structure, leading to a monoclinic distortion, which increases with the increased substitution of Bi^{3+} by Pb^{2+}. From literature reports, it was found that vacancies usually play an important role in grain growth and have a remarkable effect on electrical properties of materials, especially for electronic ceramics such as

[a]Author to whom correspondence should be addressed.

$BaTiO_3$.[22] Therefore, it is also relevant to study the effect of Pb^{+2} incorporation in the composition $Sr_xBi_{2z}Ta_2O_9$ compound in order to identify its role in the structure of this compound. In this work, we explore the correlation between the Sr deficiency in SBT films and the observed enhanced polarization from the viewpoint of defect chemistry. Based on the similar structures of $PbBi_2Ta_2O_9$ and $SrBi_2Ta_2O_9$, the effect of Pb^{2+} substitution on remanent polarization and fatigue properties of $Sr_xBi_{2y}Ta_2O_9$ composition was also investigated.

II. EXPERIMENT

The starting materials for the MOD process were bismuth 2-ethylhexanoate $[Bi(CH_3(CH_2)_3CH(C_2H_5)COO)_3]$, strontium 2-ethylhexanoate $[Sr(CH_3(CH_2)_3CH(C_2H_5)COO)_2]$, lead 2-ethylhexanoate $[Pb(CH_3(CH_2)_3CH(C_2H_5)COO)_2]$, and tantalum ethoxide $[Ta(OC_2H_5)_5]$ with 2-ethylhexanoic acid as the solvent. The metalorganic precursors were mixed to form solutions with compositions of $Sr_xPb_yBi_{2z}Ta_2O_9$. Prior to film deposition, the substrate ($Pt/Ti/SiO_2/Si$) was cleaned in acetone and alcohol ultrasonic baths, then blown dry with N_2 gas. The solutions were spin coated onto the substrate at a speed of 3000 rpm. After each coating, the as-deposited film was dried on a hot plate at a temperature of about 350 °C to remove the solvent before application of the next coating. After the process was repeated four times, the as-deposited films were sintered at 750–800 °C in air for 30 min by directly placing the coated substrate into a preheated tube furnace.

The crystal structures of the films were analyzed by using Siemens D5000 x-ray diffraction (XRD) with Cu Kα radiation and a Ni filter. The chemical composition of the films was determined using inductively coupled plasma (ICP) mass spectroscopy (Perkin Elmer, SCIEX ELAN 5000). The film thickness was measured by Dektak surface profilometer. Field-emission scanning electron microscopy Hitachi S4000) was performed to investigate the surface morphology of the films. Patterned top Au electrodes through a shadow mask on an area of $8.0\times10^{-4}\,cm^2$ area were sputter deposited onto the SBT layers to define capacitors in order to perform electrical measurements. A ferroelectric testing system (RT-66A, Radiant Technologies Inc.) operating in the virtual-ground mode was used to obtain the remanent polarization (P_r)-coercive field (E_c) hysteresis characteristics and fatigue properties. Fatigue tests of the films were conducted using a bipolar square wave of 5 V at 1 MHz.

III. RESULTS

A. $Sr_xBi_{2z}Ta_2O_9$ thin films

1. Microstructure and phase evolution

XRD analysis was used to investigate the effect of Sr content on the phase development of $Sr_xBi_2Ta_2O_9$ film ($0.5 \leqslant x \leqslant 1.2$) annealed at 800 °C for 0.5 h. As shown in Fig. 1, an unknown phase at $2\theta = 29.5°$ was observed for $Sr_{0.6}Bi_2Ta_2O_9$ film and the peak intensity increased with increasing Sr deficiency. This peak might originate from the formation of $BiTaO_4$ (JCPDS 16-0906) according to the report of Hase *et al.*[13]

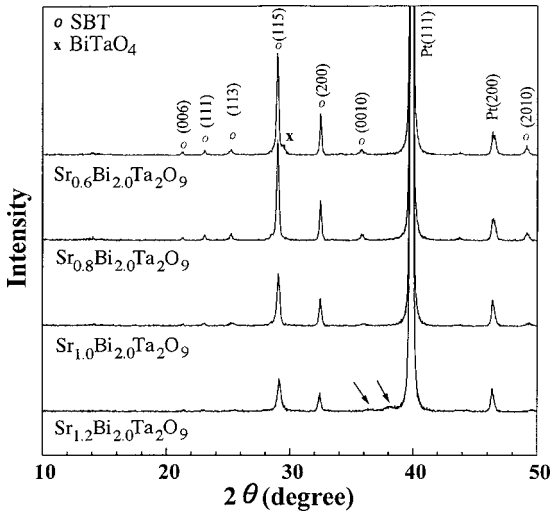

FIG. 1. XRD patterns of $Sr_xBi_2Ta_2O_9$ films annealed at 800 °C for 0.5 h.

Table I lists the chemical compositions of $Sr_xBi_2Ta_2O_9$ films annealed at 800 °C for 0.5 h. The molar numbers of Sr, Ta, and Bi in those films are very close to the compositions in the precursor solutions for Sr-deficient $Sr_xBi_2Ta_2O_9$ films. In other words, the films with Sr deficiency show no obvious Bi loss. However, for the films with Sr $(x)=1$, a partial loss of Bi was found compared to those in precursor solutions. This might indicate that the occupation of Sr vacancies by Bi cations reduces the evaporation of Bi_2O_3 or Bi loss. Similarly, for Sr-deficient $Sr_{0.8}Pb_{0.2}Bi_{2.3}Ta_2O_9$ films, except for the loss of Pb, the reduction of Bi was also observed.

The microstructure evolution of $SrBi_{2.3}Ta_2O_9$ films changes substantially as a function of Sr content, as shown in Fig. 2. The grain size is larger for Sr-deficient films than for film with stoichiometric Sr content and the Sr-rich film. The microstructure of $Sr_{0.6}Bi_{2.3}Ta_2O_9$ film presents a rod-like grain matrix interposed with a few smaller microcrystals indicated by the arrows in Fig. 2(a). The microcrystals were regarded to be the secondary phase (probably $BiTaO_4$) as inferred from the XRD patterns (Fig. 1). In addition, with increasing Sr content from Sr=0.6 to 1.2, grains become finer and rounder. The average grain sizes were measured to

TABLE I. Sr/Pb/Bi/Ta ratio normalized in Ta=2 for $Sr_xPb_yBi_{2z}Ta_2O_9$ films.

Precursor solution Sr/Pb/Bi/Ta	Films prepared at 800°C Sr/Pb/Bi/Ta
0.8/0/2.0/2	0.787/0/2.05/2
0.8/0/2.3/2	0.793/0/2.31/2
1.0/0/2.0/2	0.977/0/2.04/2
1.0/0/2.3/2	0.969/0/2.24/2
0.8/0.2/2.0/2	0.792/0.183/1.98/2
0.8/0.2/2.3/2	0.789/0.186/2.24/2
1.0/0.2/2.0/2	0.971/0.175/1.97/2
1.0/0.2/2.3/2	0.976/0.172/2.19/2

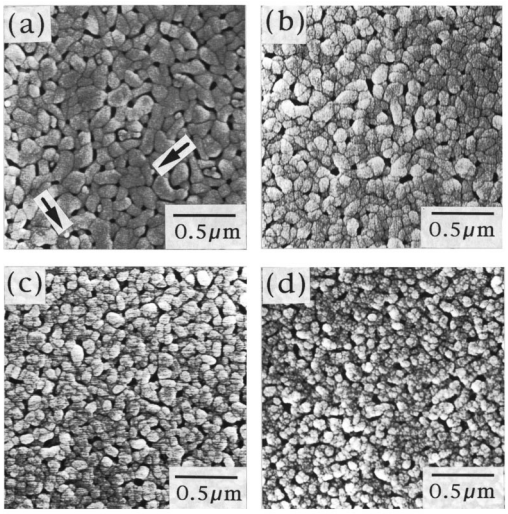

FIG. 2. Dependence of Sr content on microstructure of: (a) $x=0.6$, (b) $x=0.8$, (c) $x=1.0$, and (d) $x=1.2$ compositions in $Sr_xBi_{2.3}Ta_2O_9$ films annealed at 800 °C for 0.5 h.

be about 190, 145, 100, and 70 nm for $x=0.6$, 0.8, 1.0, and 1.2, respectively.

2. Electrical properties

Figure 3 shows the P–E hysteresis curves of both $SrBi_2Ta_2O_9$ and $Sr_{0.8}Bi_{2.3}Ta_2O_9$ films annealed at 800 °C. The $2P_r$ value of $Sr_{0.8}Bi_{2.3}Ta_2O_9$ film was measured to be about 15.9 $\mu C/cm^2$, which is larger than that of $SrBi_{2.3}Ta_2O_9$ films ($2P_r=6.7\ \mu C/cm^2$) for an applied voltage of 5 V. Here, the hysteresis curves of Sr-deficient SBT film often exhibit little horizontal shifts along the voltage axis as compared with that of stoichiometric SBT film. The P_r value was also found to be strongly dependent on Sr content in $Sr_xBi_{2.3}Ta_2O_9$ compositions for a variety of Bi content ($2y=2.0$–2.3) (Fig. 4). When the Sr content exceeded 20% ($x=1.2$), there is no hysteresis curve. However, the $2P_r$ value increased with the decrease in Sr content from Sr=1.1 to Sr=0.8 and then decreased with further decreasing Sr content from Sr=0.8 to Sr=0.6. The maximum value of $2P_r$ was obtained at the $Sr_xBi_{2.3}Ta_2O_9$ films with Sr=0.8. A similar phenomenon was also observed for the $Sr_xBi_{2.0}Ta_2O_9$ films.

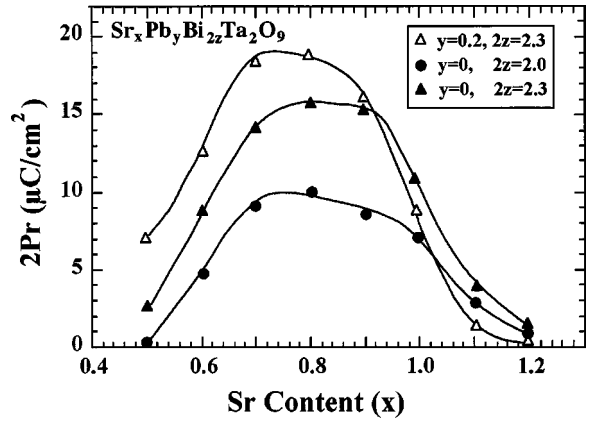

FIG. 4. Remanent polarization $2P_r$ values in $Sr_xBi_{2z}Ta_2O_9$ and $Sr_xPb_yBi_{2z}Ta_2O_9$ films fired at 800 °C for 0.5 h.

Fatigue endurance was tested with 1 MHz bipolar pulses at 5 V. Figure 5 shows the fatigue behavior of $Sr_xBi_{2z}T_2O_9$ films prepared at 800 °C for 0.5 h. Most of the $Sr_xBi_{2.3}Ta_2O_9$ films show no appreciable fatigue after 10^9 cycles. However, a partial loss of $2P_r$ after fatigue was observed for $Sr_{0.8}Bi_{2.3}Ta_2O_9$-based capacitors. The percentage of the remanent polarization after 10^9 cycles was approximately 87% of the initial value. Similar dependence of fatigue endurance on composition was also observed by Noguchi *et al.*[12]

B. $Pb_yBi_2Ta_2O_9$ thin films

Figure 6 shows the XRD patterns of $Pb_yBi_2Ta_2O_9$ (PBT) films fired at 800 °C for 0.5 h. Some peaks at $2\theta=29.4$, 32.6, and 34.1, corresponding to $BiTaO_4$ phase in $Sr_{0.6}Bi_2Ta_2O_9$ film, began to develop. Furthermore, these peak intensities increased with decreasing Pb content in $Pb_yBi_2Ta_2O_9$ films. The dependence of grain size on Pb content in PBT films was completely different from that of Sr in SBT films. As shown in Fig. 7, a fine-grained microstructure was developed in the $Pb_yBi_2Ta_2O_9$ film with Pb=0.6 and

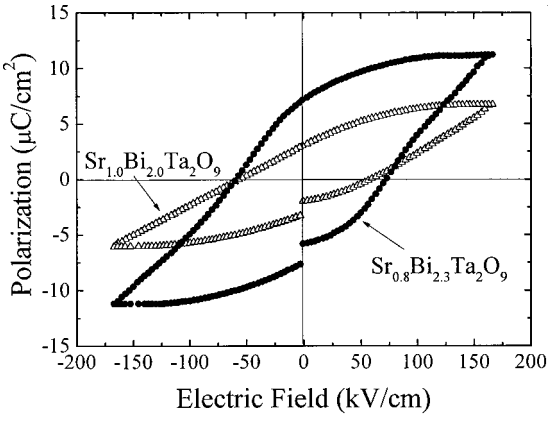

FIG. 3. P-E hysteresis loops of: (a) $SrBi_2Ta_2O_9$ and (b) $Sr_{0.8}Bi_{2.3}Ta_2O_9$ films annealed at 800 °C for 0.5 h under applied voltage of 5 V.

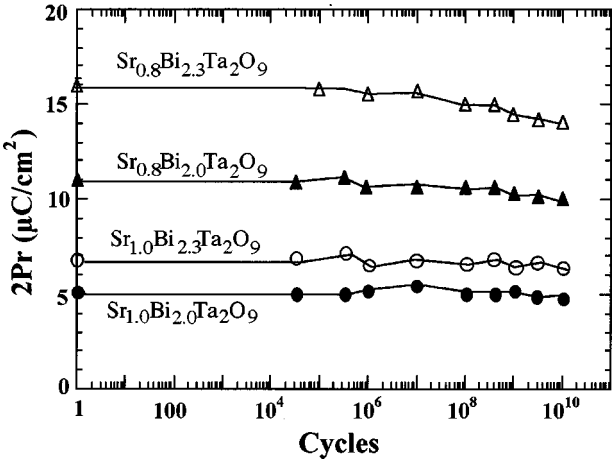

FIG. 5. Fatigue behavior of $Sr_xBi_{2z}Ta_2O_9$ films with an applied voltage of 5 V at 1 MHz.

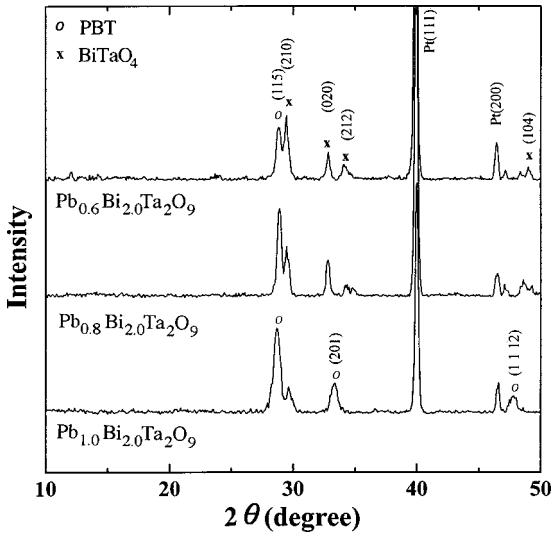

FIG. 6. XRD patterns of $Pb_yBi_2Ta_2O_9$ films annealed at 800 °C for 0.5 h.

accompanied with the formation of pores because of volume shrinkage during the amorphous/crystalline transformation. With increasing Pb content, clusters appeared [for stoichiometric PBT films, Fig. 7(c)], probably originated from a single nucleus, similar to spherulites commonly seen in amorphous-to-crystalline transitions. Some clusters with pores appear located near the center of each cluster and on the grain boundaries. Even for Pb-rich PBT films, the clusters are still seen [Fig. 7(d)].

The hysteresis curve of $Pb_yBi_2Ta_2O_9$ films with $y=0.7$ and 1.0 were further measured under an applied voltage of 5 V. The film with $y=1.0$ displayed a remanent polarization P_r of 3.3 μC/cm^2 but the remanent polarization could not be measured for Pb-deficient $Pb_yBi_2Ta_2O_9$ films such as $y=0.7$. The fatigue behavior of $PbBi_2Ta_2O_9$ films were also tested and no appreciable loss after 10^9 cycles was observed.

C. $Sr_xPb_{1-x}Bi_{2.3}Ta_2O_9$ thin films

Both $SrBi_2Ta_2O_9$ and $PbBi_2Ta_2O_9$ are Aurivillius-structure layered bismuth compounds of $(Bi_2O_2)^{2+}$ $(A_{m-1}B_mO_{3m+1})^{2-}$ with $m=2$. However, both $Sr_xBi_2Ta_2O_9$ and $Pb_yBi_2Ta_2O_9$ films have completely different microstructure evolution and electrical properties with changing A site content. The optimal remanent polarization occurs for the Sr-deficient $Sr_{0.8}Bi_{2.3}Ta_2O_9$ but a very poor polarization was observed in the Pb deficient $Pb_{0.8}Bi_{2.3}Ta_2O_9$ films. This finding suggests that the A-site atom (such as Sr or Pb) in the Aurivillius-structure layered bismuth compounds plays a very important role in the electric properties. In order to clarify the relative effect, the composition of $Sr_xPb_{1-x}Bi_{2z}Ta_2O_9$ films was chosen as a basis to compare its role in polarization and microstructure.

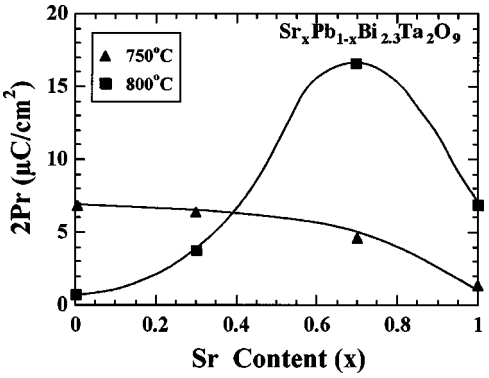

FIG. 8. Dependence of Sr content on remanent polarization of $Sr_xPb_{1-x}Bi_{2.3}Ta_2O_9$ films annealed at 750–800 °C.

When $Sr_xPb_{1-x}Bi_{2.3}Ta_2O_9$ films were annealed at 750 °C for 0.5 h, a maximum value of $2P_r$, as shown in Fig. 8, occurs at the film with $x=0$, i.e., $PbBi_{2.3}Ta_2O_9$. Moreover, as the Sr content increases, the $2P_r$ changes little up to $x=0.7$ and then a sharp drop of $2P_r$ is observed at $x=1$. When the annealing temperature was raised to 800 °C, a second phase was detected in the Pb-rich $Sr_xPb_{1-x}Bi_{2.3}Ta_2O_9$ composition as observed in Pb-deficient $Pb_yBi_{2.0}Ta_2O_9$ film (Fig. 6), therefore, causing the remanent polarization to be apparently reduced, especially for a $PbBi_{2.3}Ta_2O_9$ film. Consequently, a maximum remanent polarization ($2P_r=16.7\ \mu$C/cm^2) was obtained near the composition of $Sr_{0.7}Pb_{0.3}Bi_{2.3}Ta_2O_9$ film ($x=0.7$). In this case, the results also reflect the fact that the minor addition of Pb into $Sr_xBi_{2.3}Ta_2O_9$ films does not strongly influence the dependence of Sr content on P_r value.

In order to further clarify the role of Pb additive in $Sr_xBi_{2.3}Ta_2O_9$ films, the electrical properties and microstructural morphology of $Sr_xBi_{2.3}Ta_2O_9$ films doped with 20 mol % PbO were studied. The XRD results show that no changes in the diffraction pattern were observed except for a slight variation in the intensity of some diffraction peaks. The dependence of film morphology on Sr content in the $Sr_xPb_{0.2}Bi_{2.3}Ta_2O_9$ compositions is shown in Fig. 9. As the $Sr_{0.6}Bi_{2.3}Ta_2O_9$ film is doped with 20 mol % PbO, i.e., $Sr_{0.6}Pb_{0.2}Bi_{2.3}Ta_2O_9$, the grains begin to grow and coalesce with each other. Therefore, some large grains were formed along with finer pores located near the center of a large grain or at the grain boundaries. Obviously, the addition of PbO promotes the grain growth of $Sr_{0.6}Bi_{2.3}Ta_2O_9$ film. Furthermore, as compared with the grain size of SEM micrographs

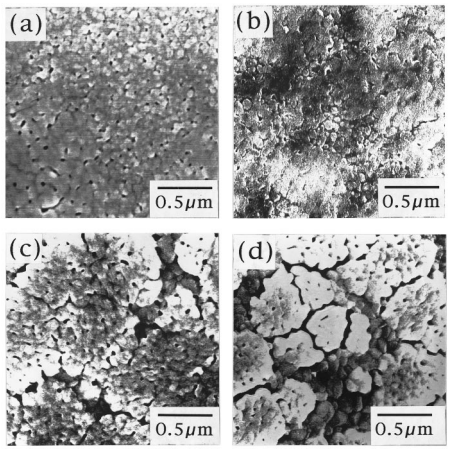

FIG. 7. SEM plan views of $Pb_yBi_2Ta_2O_9$ films with: (a) $y=0.6$, (b) $y=0.8$, (c) $y=1.0$, and (d) $y=1.3$ compositions annealed at 800 °C for 0.5 h.

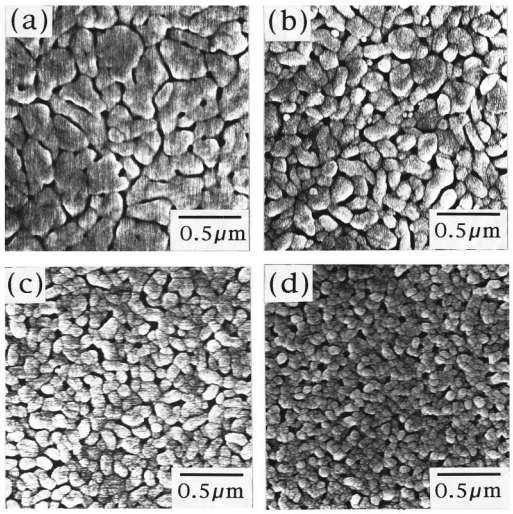

FIG. 9. SEM plan views of $Sr_xPb_{0.2}Bi_{2.3}Ta_2O_9$ films with: (a) $x=0.6$, (b) $x=0.8$, (c) $x=1.0$, and (d) $x=1.2$ compositions annealed at 800 °C for 0.5 h.

in Fig. 2 for $Sr_xBi_{2.3}Ta_2O_9$ films, a larger-grain microstructure was obtained for $Sr_xPb_{0.2}Bi_{2.3}Ta_2O_9$ films. The average grain size of $Sr_xPb_{0.2}Bi_{2.3}Ta_2O_9$ films, similar to $Sr_xBi_{2.3}Ta_2O_9$ compositions, decreases with the increase of Sr content. The average grain size was measured to be around 210 nm at the compositions of $x=0.8$ and 150 nm at $x=1.0$.

In order to compare the effect of 20 mol % PbO on the remanent polarization of $Sr_xBi_{2.3}Ta_2O_9$ films, the $2P_r$ values of $Sr_xPb_{0.2}Bi_{2.3}Ta_2O_9$ films were measured at 5 V. As shown in Fig. 4, the film with 20% Sr deficiency ($x=0.8$) still gives a maximum $2P_r$ of 19.2 $\mu C/cm^2$ for $Sr_xPb_{0.2}Bi_{2.3}Ta_2O_9$ compositions. Figure 10 shows the fatigue behavior of $Sr_xPb_{0.2}Bi_{2.3}Ta_2O_9$ films excited with 5 V pulses. The fatigue of $Sr_{0.8}Bi_{2.3}Ta_2O_9$ film is also placed in Fig. 10 for comparison. Most of the $Sr_xPb_{0.2}Bi_{2.3}Ta_2O_9$ films exhibit good fatigue endurance except for $Sr_{0.6}Pb_{0.2}Bi_{2.3}Ta_2O_9$ films having a slight degradation of 9%. The fatigue endurance of $Sr_{0.8}Bi_{2.3}Ta_2O_9$ film was obviously enhanced by 20 mol % PbO additions.

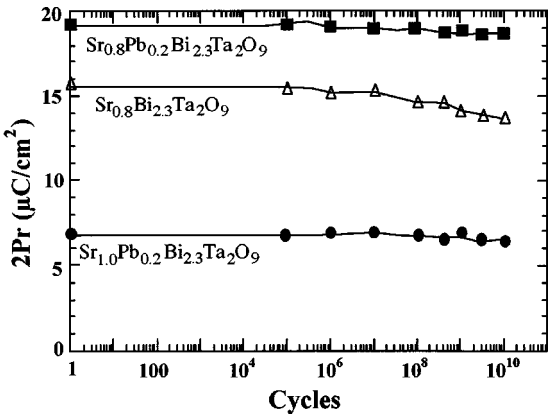

FIG. 10. Effect of 20 mol % Pb additive on the fatigue characteristics of $Sr_xBi_{2.3}Ta_2O_9$ films under applied voltage of 5 V.

IV. DISCUSSION

A. Microstructure and polarization properties

The $2P_r$ values increased with the decrease in Sr content from Sr=1.1 to Sr=0.8 for $Sr_xBi_{2.3}Ta_2O_9$ films annealed at 800 °C. The enhanced P_r could be attributed to the grain growth and grain orientation as reported in the literature.[12–14] However, in our case, no preferred orientation was observed in the XRD pattern for $Sr_xBi_{2.3}Ta_2O_9$ films, but the microstructure of Fig. 2 indeed revealed a grain morphology transitioned from rod- to round-like as the Sr content increased. For Sr-deficient $Sr_xBi_{2.3}Ta_2O_9$ compositions, the $BiTaO_4$ phase was identified according to the XRD analysis of Fig. 1. Furthermore, the number of Sr defects would increase with the decrease in Sr content and therefore, the probability of domain pinning would increase, resulting in a reduced $2P_r$. Although the $Sr_{0.6}Bi_{2.3}Ta_2O_9$ film has larger grain size, both Sr vacancy concentration and second phase formation of $BiTaO_4$ microcrystals overcame the grain-size effect. Therefore, a maximum polarization was obtained at Sr=0.8 for both $Sr_xPb_{0.2}Bi_{2.3}Ta_2O_9$ and $Sr_xBi_{2.3}Ta_2O_9$ films. The enhanced remanent polarization of the former composition could be attributed to the larger grain size compared to the latter composition without Pb.

As compared to $SrBi_2Ta_2O_9$, the $PbBi_2Nb_2O_9$ ceramic has a lower crystallization temperature and sintering temperature. Therefore, at the lower annealing temperature of 750 °C, Pb-rich composition (i.e., $x=0$) in $Sr_xPb_{1-x}Bi_{2.3}Ta_2O_9$ ($0<x<1$) films gives a larger remanent polarization as compared to the film with $x=1$. At 800 °C, however, a second phase was observed in the Pb-rich films as shown in the XRD pattern of Fig. 6 for $PbBi_2Ta_2O_9$ composition, and thus, the remanent polarization was strongly reduced for increasing Pb content (or decreasing Sr content). An optimal $2P_r$ of 16.7 $\mu C/cm^2$ was attained around the composition of $Sr_{0.7}Pb_{0.3}Bi_{2.3}Ta_2O_9$. Here, further increasing Sr content leads to the decrease of remanent polarization since grain size was remarkably reduced.

B. Role of Pb in $Sr_xPb_yBi_{2z}Ta_2O_9$ films

From electronic structure, both Pb and Bi have a lone pair of out-shell electrons of $6s^2$. This chemical aspect could be significant since the lone-pair electrons of Pb and Bi are known to have a large polarizability and to promote strong ferroelectricity. However, from the viewpoint of ferroelectricity, Pb in $PbBi_2Ta_2O_9$, as similar to Sr in $SrBi_2Ta_2O_9$, i.e., it occupies the A site in Aurivillius compounds and the radii of Pb (1.18 Å), Sr (1.16 Å) and Bi (1.02 Å) are very close.[23] It will be interesting to study the role of Pb in $SrBi_2Ta_2O_9$ film in order to identify the key chemical and structural elements that lead to optimal polarization and polarization fatigue.

Assuming Pb can completely substitute for Sr in the $SrBi_2Ta_2O_9$ composition, the $PbBi_2Ta_2O_9$ film should display a specific ferroelectricity. However, since PbO, after being annealed at high temperature, is easily evaporated, the $PbBi_2Ta_2O_9$ composition probably became $Pb_zBi_2Ta_2O_9$ ($z<1$). Furthermore, if the role of Pb is similar to Sr, the measured polarization of $Pb_zBi_2Ta_2O_9$ film should have been

comparable with that of $Sr_xBi_2Ta_2O_9$ ($x<1$) films. However, there was no appreciable polarization observed for Pb-deficient films such as $Pb_{0.7}Bi_2Ta_2O_9$. Obviously, the role of Pb content in PBT film in polarization and microstructure is completely different from that of Sr in $Sr_xBi_{2.3}Ta_2O_9$ film.

With the addition of 20 mol % PbO, the dependence of grain size on Sr content in $Sr_xPb_{0.2}Bi_{2.3}Ta_2O_9$ films shows similar tendency as the $Sr_xBi_{2.3}Ta_2O_9$ films. However, we found that the grain size of $Sr_{0.8}Pb_{0.2}Bi_{2.3}Ta_2O_9$ film (Fig. 9) was larger as compared with $Sr_{0.8}Bi_{2.3}Ta_2O_9$ film (Fig. 2). This observation indicates that the incorporation of PbO plays an important role in promoting grain growth of $Sr_{0.8}Bi_{2.3}Ta_2O_9$ film. That is the reason why the remanent polarization of $Sr_{0.8}Pb_{0.2}Bi_{2.3}Ta_2O_9$ film is enhanced compared to $Sr_{0.8}Bi_{2.3}Ta_2O_9$ film. According to the defect chemistry, if the ionic defects were produced and the overall electroneutrality was kept, the substitution of Pb^{2+} for Bi^{3+} will create oxygen vacancies as follows:

$$2\,PbO \xrightarrow{Bi_2O_3} 2\,Pb'_{Bi} + V_o^{\bullet\bullet} + 2O_o^x, \tag{1}$$

As reported for $BaTiO_3$ ceramics, the grain growth was usually observed with increasing acceptor concentrations because oxygen vacancies will be produced.[22] These phenomena reflected that the small amount of Pb was probably incorporated into the Bi site in the $Sr_{0.8}Pb_{0.2}Bi_{2.3}Ta_2O_9$ films.

C. Fatigue behavior of $Sr_{1-x}Pb_xBi_{2.3}Ta_2O_9$ films

Ferroelectric thin films of bismuth-containing layered perovskite such as $SrBi_2Ta_2O_9$ and $SrBi_2Nb_2O_9$ have been reported to have excellent good fatigue resistance. In our results, although Sr-deficient $SrBi_{2.3}Ta_2O_9$ film shows an optimal remanent polarization of $2P_r=15.9\,\mu C/cm^2$, a loss of Pr of 15% was measured after 10^9 cycles. A similar phenomenon was also reported by Noguchi *et al.*[12] In contrast, the $SrBi_{2.3}Ta_2O_9$ or $SrBi_2Ta_2O_9$ films show no appreciable polarization loss under the same applied voltage of 5 V.

There are several proposals that attempt to explain the fatigue behavior of ferroelectric thin films especially for piezoelectric transducers (PZTs). These proposals are all related to defects, which may be trapped at domain boundaries to lower their mobility. However, there have been different views of the species of the defects and the location of the trapping sites. Oxygen vacancy and electron/hole injection have been suggested as possible mechanisms for the fatigue of PZT films.[24,25] Support for the oxygen vacancy model was drawn from the observation that oxygen vacancy was produced in PZT film because PbO was easily evaporated during high temperature annealing. In our case, however, the $Sr_{0.8}Bi_{2.3}Ta_2O_9$ film prepared with both 20 mol % deficiency Sr and 15 mol % excess Bi should have very few oxygen vacancies. Therefore, the oxygen vacancy mechanism is not applicable in explaining the fatigue behavior of $Sr_{0.8}Bi_{2.3}Ta_2O_9$ film. In the other model, the electron/hole mechanism states that the injection of charge carrier (mainly electrons) will be trapped at domain boundaries to pin domains. The tendency for this to occur increases when the material is donor doped.[25] For $Sr_{0.8}Bi_{2.3}Ta_2O_9$ film, it was considered that Sr deficiency was compensated by excess Bi since both radius of Sr (1.16 Å) and Bi (1.02 Å) are very close.[11,26] The electron can be produced by substituting Bi for Sr vacancy according to the defect reaction as follows:

$$Bi_2O_3 \xrightarrow{2SrO} 2Bi_{Sr}^{\bullet} + 2O_o^x + 2e^-. \tag{2}$$

With 15 mol % excess Bi, the Sr-deficient $Sr_{0.8}Bi_{2.3}Ta_2O_9$ film is probably considered as donor doped and the chance for electron injection is high. Therefore, after cycling, the injected electron was trapped by the ions Bi_{Sr}^{*}, which in turn could pin the domain boundary movement, causing the switchable polarization to decrease. This is in agreement with our fatigue data shown in Fig. 5. Furthermore, the number of Sr defects would increase with the decrease in Sr content and therefore, cause a larger coercive field to polarize the film.

Although Pb is a volatile species, the anion (oxygen) vacancies accompanied by the substitution of Pb for Bi do not seem to adversely affect the fatigue resistance as evidenced in Fig. 10. This gives clearer evidence to rule out the oxygen vacancy mechanism for fatigue that has been proposed for PZT films.[24] According to the fatigue model proposed by Warren *et al.*[25] and Eq. (2), the released electronic charge trapping at domain walls can inhibit the domain motion and lead to the partial suppression of the switchable polarization in $Sr_{0.8}Bi_{2.3}Ta_2O_9$ film. However, as indicated in Table I, $Sr_{0.8}Bi_{2.3}Ta_2O_9$ film shows almost no loss of Bi, but the addition of Pb induces the reduction of Bi in the $Sr_{0.8}Pb_{0.2}Bi_{2.3}Ta_2O_9$ film. It is plausible for Pb to occupy the Sr vacancies and produce free Bi which will be readily evaporated from the surface because of the high vapor pressure of Bi at high temperatures. Therefore, the reaction in Eq. (2) is probably partially inhibited by doping Pb into the $Sr_{0.8}Bi_{2.3}Ta_2O_9$ film so that the electronic charge cannot be easily released. Alternatively, the released electrons due to the Bi substitution for Sr can be possibly compensated from the hole or oxygen vacancies produced from the substitution of Pb for Bi as shown in Eq. (1). Consequently, the fatigue behavior of $Sr_{0.8}Pb_{0.2}Bi_{2.3}Ta_2O_9$ film can be improved by incorporating 20 mol % PbO into $Sr_{0.8}Bi_{2.3}Ta_2O_9$ film.

V. CONCLUSIONS

$Sr_xBi_{2.3}Ta_2O_9$ and $Pb_yBi_{2.3}Ta_2O_9$ films have shown completely different dependence of microstructure evolution and ferroelectric properties on A site (Sr or Pb) content in Aurivillius compounds of $(Bi_2O_2)^{2+}$ $(A_{m-1}B_mO_{3m+1})^{2-}$.

Ferroelectric properties of $Sr_xBi_{2.3}Ta_2O_9$ films could be further enhanced by the addition of 20 mol % Pb.

The addition of Pb is responsible for the enhanced grain growth in $Sr_{0.8}Pb_{0.2}Bi_{2.3}Ta_2O_9$ films.

Fatigue endurance of $Sr_{0.8}Bi_{2.3}Ta_2O_9$ films in this study become problematic after 10^9 cycles with decreasing Sr content. This was proposed to originate from with electron injection and traps due to the occupation of Bi for Sr vacancies.

Fatigue behavior of $Sr_{0.8}Bi_{2.3}Ta_2O_9$ film can be improved by incorporating 20 mol % PbO because the release of electronic charge could be partially inhibited by doping Pb to occupy the Sr vacancies.

ACKNOWLEDGMENT

The authors gratefully acknowledge financial support by the National Science Council of the Republic of China through Contract No. NSC87-2218-E-009-016.

[1] G. A. Smolenskii, V. A. Isupov, and A. I. Agranovskaya, Sov. Phys. Solid State **1**, 149 (1959).
[2] G. A. Smolenskii, V. A. Isupov, and A. I. Agranovskaya, Sov. Phys. Solid State **3**, 651 (1961).
[3] C. A. Paz de Araujo, J. D. Cuchiaro, M. C. Scott, L. D. McMillan, and J. F. Scott, Nature (London) **374**, 627 (1995).
[4] O. Auciello, J. F. Scott, and R. Ramesh, Phys. Today, 22 (1998).
[5] H.-M. Tsai, P. Lin, and T. Y. Tseng, Appl. Phys. Lett. **72**, 1787 (1998).
[6] R. Dat, J. K. Lee, O. Auciello, and A. I. Kingon, Appl. Phys. Lett. **67**, 572 (1995).
[7] Y. Zhu, S. B. Deau, T. Li, S. Ramanathan, and M. Nagata, J. Mater. Res. **12**, 783 (1997).
[8] Y. Ito, M. Ushikubo, S. Yokoyama, H. Matsunaga, T. Atsuki, T. Yonezawa, and K. Ogi, Integr. Ferroelectr. **14**, 123 (1997).
[9] T. Hayashi, H. Takahashi, and T. Hara, Jpn. J. Appl. Phys., Part 1 **35**, 4952 (1996).
[10] I. Koiwa, T. Kanehara, J. Mita, T. Iwabuchi, T. Osaka, and S. Ono, Jpn. J. Appl. Phys. **36**, 1597 (1997).
[11] T. Atsuki, N. Soyama, T. Yonezawa, and K. Ogi, Jpn. J. Appl. Phys., Part 1 **34**, 5096 (1995).
[12] T. Noguchi, T. Hase, and Y. Miyasaka, Jpn. J. Appl. Phys., Part 1 **35**, 4900 (1996).
[13] T. Hase, T. Noguchi, K. Amanuma, and Y. Miyasaka, Integr. Ferroelectr. **15**, 127 (1997).
[14] K. Watanabe, M. Tanaka, E. Sumitomo, K. Katori, H. Yagi, and J. F. Scott, Appl. Phys. Lett. **73**, 126 (1998).
[15] T. Hayashi, H. Takahashi, and T. Hara, Jpn. J. Appl. Phys., Part 1 **35**, 4952 (1996).
[16] P. Y. Chu, R. E. Jones, P. Zurcher, D. J. Taylor, B. Jiang, S. J. Gillespie, and Y. T. Li, J. Mater. Res. **11**, 1065 (1996).
[17] H. Watanabe, T. Mihara, H. Yoshmori, and C. A. Paz de Araujo, Jpn. J. Appl. Phys., Part 1 **34**, 5240 (1995).
[18] B. Aurivillius, Ark. Kemi **1**, 463 (1949).
[19] E. C. Subbarao, Phys. Chem. Solids **23**, 665 (1962).
[20] J. Franco and G. Shirane, *Ferroelectric Crystals* (Pergamon, New York, 1962), p. 274.
[21] P. Millan and A. Castro, Mater. Res. Bull. **28**, 117 (1993).
[22] D. M. Smyth, Prog. Solid State Chem. **15**, 145 (1984).
[23] R. D. Shannon and C. T. Prewitt, Acta Crystallogr., Sect. B: Struct. Crystallogr. Cryst. Chem. **25**, 925 (1969).
[24] I. K. Yoo and S. B. Desu, Integr. Ferroelectr. **3**, 365 (1993).
[25] W. L. Warren, D. Dimos, B. A. Tuttle, R. D. Nasby, and G. E. Pike, Appl. Phys. Lett. **65**, 1018 (1994).
[26] M. A. Rodriguez, T. J. Boyle, B. A. Hernandez, C. D. Buchheit, and M. O. Eatough, J. Mater. Res. **11**, 2282 (1996).